ELSEVIER

Engineering Analysis with Boundary Elements 28 (2004) 919–926

ENGINEERING ANALYSIS *with* BOUNDARY ELEMENTS

www.elsevier.com/locate/enganabound

Micro-mechanical analysis of composite materials by BEM

Qing-Sheng Yang[a,*], Qing-Hua Qin[b,c]

[a]*Department of Engineering Mechanics, Numerical Simulation Center for Engineering, Beijing Polytechnic University, Beijing 100022, People's Republic of China*

[b]*Department of Mechanics, Tianjin University, Tianjin 300072, People's Republic of China*

[c]*Department of AMME, The University of Sydney, Sydney, NSW 2006, Australia*

Received 30 October 2002; revised 15 January 2003; accepted 17 January 2003

Available online 3 September 2003

Abstract

Applications to composites of a unit-cell model in conjunction with boundary element method (BEM) for determining their effective mechanical properties are discussed in this paper. The composite considered here consists of inclusion and matrix phases. A unit-cell model for composites with periodically distributed inhomogeneities is developed and introduced into a boundary element formulation to provide an effective means for estimating overall material constants of two-phase composites. In this model, the volume average stress and strain is calculated by the boundary tractions and displacements of the unit-cell and the periodic conditions of the composite are expressed by the periodic boundary conditions of the unit-cell. Thus BEM is suitable for performing calculations on average stress and strain fields of such composites. Numerical results for a two-phase composite with circular rigid inclusions are presented to illustrate the application of the proposed unit-cell boundary element formulation.

© 2003 Elsevier Ltd. All rights reserved.

Keywords: Composite; Effective property; Boundary element method; Micro-mechanics

1. Introduction

The composite material considered in this work consists of inhomogeneities and matrix phases. The determination of its effective properties has received considerable attention. It is well known that the effective properties of such composites depend on the physics and geometry of the two phases. For estimating the effective properties of the composite, the equivalent inclusion method is a popular approach. It is based on Eshelby's eigenstrain solution for single inclusions embedded into infinite matrix [1] and the effective properties can be expressed in terms of the volume fraction and geometries of the inclusion as well as the properties of the components. Over recent years various methods have been developed based on this approach and have been used widely in determining the overall properties of various composite materials [2–4].

The concept of a unit-cell, or representative volume element (RVE) in other words, has been widely applied in the analysis of composite materials with periodic microstructure [5–8]. The composite is an assembled body with a periodic RVE. A unit-cell or RVE is a repeatable cell of composite material. Its statistical characters, for example, the volume fraction, are taken to be the same as those measured in the whole composite. Fig. 1 shows the periodic microstructure and a RVE of composites considered. Earlier investigation has focused on the approximate analytical solutions of isolated concentric cylinders for unidirectional fiber composites [2,5]. However, very limited analytical solutions can be obtained due to the difficulties for direct mathematical description of the displacement fields in the composite cylinder. This is particularly true for a problem with complexity in the aspects of geometry and mechanical deformation. A combination of the micro-mechanics models used in Refs. [2,5] and numerical methods such as the finite element (FE) and boundary element (BE) methods provides a powerful computational tool for estimating the effective material properties of such composites. It should be mentioned that the main disadvantage of the FE method is that domain discretization is required in order to perform the analysis. Moreover, in some cases it results in both an inaccurate and an expensive technique, especially in solving

* Corresponding author. Tel.: +86-10-67392760; fax: +86-10-67391617.

E-mail address: qsyang@bjpu.edu.cn (Q.-S. Yang).

0955-7997/03/$ - see front matter © 2003 Elsevier Ltd. All rights reserved.
doi:10.1016/S0955-7997(03)00118-8

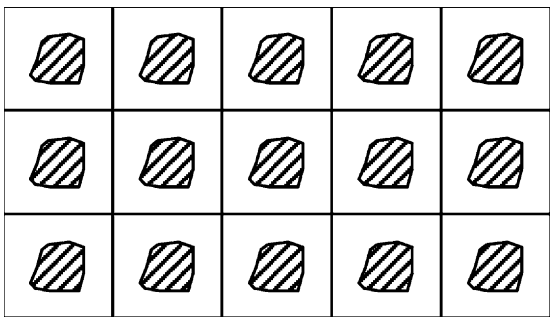

Fig. 1. A composite with periodic cells.

inclusion-matrix problems. On the other hand, the BE method involves discretization of the boundary of a structure only, because the governing differential equation is satisfied exactly inside the domain, leading to a relatively smaller system size with sufficient accuracy. During the past decade such combinations have been used for estimating the effective properties of composites with fibers, particulates or cracks [6–8]. The numerical method used in most studies for this purpose is the FE method. However, the simple, accurate and economic features of boundary element method (BEM) can make prediction more efficient [9–13], because the volume average procedure of the local fields requires information about the boundary of the RVE only. In this paper, a numerical approach for determining the overall material properties of two-phase composites is presented. This approach is based on a proposed unit-cell model and BEM. The energy equivalence principle [5], which is based on the assumption that the strain energy stored in both media (the real and the homogenized one) is equal, is used to provide equations for determining effective material constants. Numerical results for a two-phase composite with rigid circular inclusions are presented to illustrate the application of the proposed unit-cell BE approach.

2. The unit-cell model

The unit-cell model considered in this paper, shown in Fig. 2, is an infinite two-phase composite containing periodically distributed inhomogeneities, which may be cracks, holes, fibers, etc. In the model, a RVE Ω is chosen so as to be statistically representative of the two-phase composite. In particular, the characteristic size of the heterogeneities is

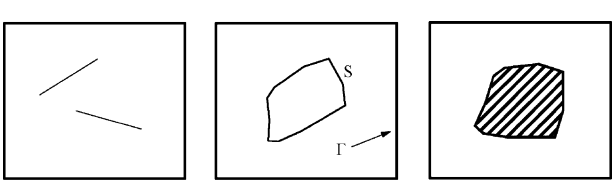

(a) crack (b) hole (c) fiber

Fig. 2. Unit-cell (or RVE) model.

supposed to be small with respect to the dimension of the RVE, which in turn is supposed to be small compared to the wavelength of the macroscopic structure.

In order to understand the key point of the homogenization procedure, let us consider a RVE consisting of the matrix material and inclusion phase. As a RVE is comprised of different materials, the micro-constitutive law that governs each material or phase in a RVE is given by the standard elastic constitutive law. On the other hand, the macro-stress and macro-strain on the macro-level are directly associated with the global analysis of a two-phase composite. On the macro-level, a RVE is regarded just as a point with a homogenized constitutive law. The macro-stress, $\bar{\sigma}_{ij}$, is usually defined as the volume average stress in a RVE, $\langle\sigma_{ij}\rangle$, as follows

$$\bar{\sigma}_{ij} = \langle\sigma_{ij}\rangle_\Omega = \frac{1}{V}\int_\Omega \sigma_{ij}\,\mathrm{d}\Omega \tag{1}$$

where Ω is the domain of the RVE and V is its volume. Similarly, the volume average strain $\bar{\varepsilon}_{ij}$ and strain-energy density $\bar{w}$ in a RVE are defined by

$$\bar{\varepsilon}_{ij} = \langle\varepsilon_{ij}\rangle_\Omega = \frac{1}{V}\int_\Omega \varepsilon_{ij}\,\mathrm{d}\Omega \tag{2}$$

$$\bar{w}=\frac{1}{V}\int_\Omega w\,\mathrm{d}\Omega=\frac{1}{V}\int_\Omega \frac{1}{2}\sigma_{ij}\varepsilon_{ij}\,\mathrm{d}\Omega$$
$$=\frac{1}{V}\int_\Omega \frac{1}{2}D_{ijkl}\varepsilon_{ij}\varepsilon_{kl}\,\mathrm{d}\Omega=\frac{1}{V}\int_\Omega \frac{1}{2}C_{ijkl}\sigma_{ij}\sigma_{kl}\,\mathrm{d}\Omega \tag{3}$$

where $w=\sigma_{ij}\varepsilon_{ij}/2$ is density of strain energy, D_{ijkl} are local stiffness coefficients and $C_{ijkl}(\mathbf{C}=\mathbf{D}^{-1})$ are local compliant coefficients which are different from phase to phase. Moreover, the macroscopic strain energy should satisfy

$$\bar{w}=\frac{1}{2}\bar{\sigma}_{ij}\bar{\varepsilon}_{ij} \tag{4}$$

The effective properties represented by effective stiffness $\bar{D}_{ijkl}$ or compliancy $\bar{C}_{ijkl}$ of the composites can be defined by the average stress and strain

$$\bar{\sigma}_{ij}=\bar{D}_{ijkl}\bar{\varepsilon}_{kl},\quad \bar{\varepsilon}_{ij}=\bar{C}_{ijkl}\bar{\sigma}_{kl} \tag{5}$$

or by equivalence of the strain energy

$$\frac{1}{2}\bar{\sigma}_{ij}\bar{\varepsilon}_{ij}=\frac{1}{V}\int_\Omega \frac{1}{2}\sigma_{ij}\varepsilon_{ij}\,\mathrm{d}\Omega \tag{6}$$

or

$$\frac{1}{2}\bar{D}_{ijkl}\bar{\varepsilon}_{ij}\bar{\varepsilon}_{kl}=\frac{1}{V}\int_\Omega \frac{1}{2}D_{ijkl}\varepsilon_{ij}\varepsilon_{kl}\,\mathrm{d}\Omega \tag{7}$$

The linearity of stress–strain relation for elastic body leads to

$$\bar{D}_{ijkl}=\frac{\partial^2\bar{w}}{\partial\bar{\varepsilon}_{ij}\,\partial\bar{\varepsilon}_{kl}} \tag{8}$$

Then an explicit form of the effective stiffness components can be obtained [14].

The effective quantities of the stress, strain and strain energy can be calculated by corresponding boundary values with surface average procedures. For the case of small strain, we have

$$\varepsilon_{ij} = \frac{1}{2}(u_{i,j} + u_{j,i}) \tag{9}$$

where u_i are displacement components. Applying the divergence theorem in Eq. (2) yields

$$\bar{\varepsilon}_{ij} = \frac{1}{V}\int_{\Omega} \varepsilon_{ij}\,\mathrm{d}\Omega = \frac{1}{2V}\int_{\Gamma}(u_i n_j + u_j n_i)\mathrm{d}\Gamma \tag{10}$$

where Γ is the boundary of the RVE, and n_i is the outward normal vector on boundary Γ.

By using the divergence theorem, the volume average stresses in Eq. (1) can also be expressed as

$$\bar{\sigma}_{ij} = \frac{1}{V}\int_{\Omega} \sigma_{ij}\,\mathrm{d}\Omega = \frac{1}{2V}\int_{\Gamma}(T_i x_j + T_j x_i)\mathrm{d}\Gamma \tag{11}$$

where x_i are Cartesian coordinates, T_i are the traction components acting on the surface of the RVE. It is found from Eq. (11) that the volume average stresses are related only to the tractions on the boundary of the RVE.

Let us consider, for illustration, the RVE shown in Fig. 3. The volume average stress can be obtained as

$$\bar{\sigma}_{11} = \frac{1}{b}\int_{\mathrm{BC}} \sigma_{11}\,\mathrm{d}\Gamma, \qquad \bar{\sigma}_{22} = \frac{1}{a}\int_{\mathrm{DC}} \sigma_{22}\,\mathrm{d}\Gamma \tag{12a}$$

$$\bar{\sigma}_{12} = \bar{\sigma}_{21} = \frac{1}{b}\int_{\mathrm{BC}} \sigma_{12}\,\mathrm{d}\Gamma = \frac{1}{a}\int_{\mathrm{DC}} \sigma_{21}\,\mathrm{d}\Gamma \tag{12b}$$

Using the definitions described above, the following three types of boundary condition are usually used to evaluate the overall material properties [15,16].

(a) Uniform traction σ^0_{ij} on the boundary Γ of the RVE:

$$T_i = \sigma_{ij} n_j = \sigma^0_{ij} n_j \tag{13}$$

In this case, we have $\bar{\sigma}_{ij} = \sigma^0_{ij}$ and $\bar{\varepsilon}_{ij} = \bar{C}_{ijkl}\sigma^0_{kl}$.

(b) Uniform displacement on the boundary Ω of the RVE. The component of a displacement vector in the RVE, u_i, is given as

$$u_i = \varepsilon^0_{ij} x_j \tag{14}$$

In this case, we have $\bar{\varepsilon}_{ij} = \varepsilon^0_{ij}$ and $\bar{\sigma}_{ij} = \bar{D}_{ijkl}\varepsilon^0_{kl}$.

(c) Periodic condition on the boundary ∂V of the RVE

$$u_i = \varepsilon^0_{ij} x_j + u^0_i \tag{15}$$

where n_j are components of the outer normal unit vector, x_j are space coordinates, and u^0_i is periodic and represents the fluctuation part of the displacement.

In addition, average strain energy can be expressed by the boundary values according to the work-energy principle

$$\bar{w} = \frac{1}{V}\int_{\Omega} \frac{1}{2}\sigma_{ij}\varepsilon_{ij}\,\mathrm{d}\Omega = \frac{1}{V}\int_{\Gamma} T_i u_i\,\mathrm{d}\Gamma \tag{16}$$

Therefore, the volume average of stress, strain and strain energy can be calculated by either volume or surface average processes. Once two of the three quantities are found, then the effective properties of the composites can be predicted from Eq. (5) to (8).

The volume average of stress, strain and strain energy can also be expressed by the phase volume fractions and the corresponding volume average value of each phase. For an n-phase composite, the stress, strain and strain energy can be expressed by

$$\bar{\sigma}_{ij} = \sum_{i=1}^{n} v_i \bar{\sigma}^{(i)}_{ij}, \quad \bar{\varepsilon}_{ij} = \sum_{i=1}^{n} v_i \bar{\varepsilon}^{(i)}_{ij}, \quad \bar{w}_{ij} = \sum_{i=1}^{n} v_i \bar{w}^{(i)}_{ij} \tag{17}$$

where superscript (i) stands for the variable associated with ith phase of the composite, and v_i is volume fraction of the ith phase.

From the homogenization procedure of field quantities and the definition of the effective properties described above, we can see that the traction and displacement on the boundary of the RVE are sufficient for calculating the effective properties of the composite. Thus the BEM is suitable for determining the microscopic fields in RVE.

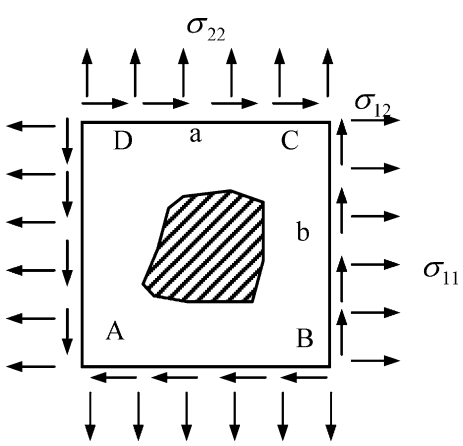

Fig. 3. Traction condition of RVE.

3. Boundary element equations

Let us consider a linear elastic RVE (Fig. 2) occupying the region Ω with boundary Γ. Further, let $\Omega^{(1)}$ be the region of the matrix and $\Omega^{(2)}$ the region occupied by the inhomogeneities. The boundary element formulation for such an RVE is in a different form for different inhomogeneities (Fig. 2). They are described below.

3.1. Cracks

It is well known that a crack can be modeled by a distributed displacement dislocation along the crack. As a consequence, the displacement dislocation can be taken as a basic variable in BE calculation. The fundamental solution for an infinite plane subjected to an edge dislocation (b_1, b_2)

at point (x_{10}, x_{20}) can be found in the Chapter 2 of Ref. [17]

$$\chi = -4H(\kappa)G(x_{220}b_1 - x_{110}b_2)\ln r_1 \tag{18}$$

where χ is the Airy stress function, $H(\kappa) = 1/2\pi(\kappa+1)$, G is the shear modulus of the material, $\kappa = 3 - 4\mu$ for plane strain and $\kappa = (3-\mu)/(1+\mu)$ for plane stress, μ being the Poisson's ratio. $x_{110} = x_1 - x_{10}$, $x_{220} = x_2 - x_{20}$, $r_1^2 = x_{110}^2 + x_{220}^2$. The related stresses and displacements can be evaluated by the following relations

$$\sigma_{11} = \chi_{,22}, \qquad \sigma_{12} = -\chi_{,12}, \qquad \sigma_{22} = \chi_{,11} \tag{19a}$$

$$\begin{aligned} 2Gu_1 &= -\chi_{,1} + (\kappa+1)P, \\ 2Gu_2 &= -\chi_{,2} + (\kappa+1)Q \end{aligned} \tag{19b}$$

where a comma followed by an argument stands for differentiation.

The functions P and Q are given by [17]:

$$P = 4H(\kappa)G\left[b_1 \tan^{-1}\left(\frac{x_{220}}{x_{110}}\right) + b_2 \ln r_1\right] \tag{20a}$$

$$Q = 4H(\kappa)G\left[b_2 \tan^{-1}\left(\frac{x_{220}}{x_{110}}\right) - b_1 \ln r_1\right] \tag{20b}$$

Using definitions defined above, expressions for u_i and σ_{ij}, due to an edge dislocation (b_1, b_2) applied at (x_{10}, x_{20}) of the material can be written in the form

$$\begin{aligned} \begin{Bmatrix} u_1 \\ u_2 \end{Bmatrix} &= \begin{bmatrix} U_{11} & U_{12} \\ U_{21} & U_{22} \end{bmatrix} \begin{Bmatrix} b_1 \\ b_2 \end{Bmatrix}, \\ \begin{Bmatrix} \sigma_{11} \\ \sigma_{12} \\ \sigma_{22} \end{Bmatrix} &= \begin{bmatrix} V_{111} & V_{112} \\ V_{121} & V_{122} \\ V_{221} & V_{222} \end{bmatrix} \begin{Bmatrix} b_1 \\ b_2 \end{Bmatrix} \end{aligned} \tag{21}$$

in which U_{ij} and V_{ijk} are easily derived from Eq. (18) to (20), and we omit those details here.

With the solution described above the boundary formulation can be developed based on the potential variational principle.

Let us consider a region Ω bounded by $\Gamma(= \Gamma_t + \Gamma_u + L)$, as shown in Fig. 4. For stationary behavior in the absence of body forces, the boundary value problem to be considered is stated as

$$\sigma_{ij,j} = 0 \qquad \text{on } \Omega \tag{22}$$

$$t_{ni} = \sigma_{ij}n_j = \bar{t}_{ni} \qquad \text{on } \Gamma_t \tag{23}$$

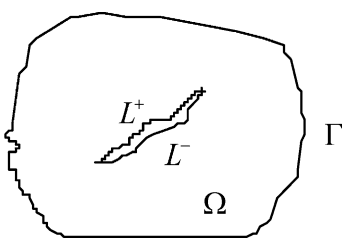

Fig. 4. Configuration of cracked solid for BEM analysis.

$$u_i = \bar{u}_i \qquad \text{on } \Gamma_u \tag{24}$$

$$t_{ni}|_{L^+} = -t_{ni}|L^- = 0 \qquad \text{on } L \tag{25}$$

where Γ_t and Γ_u are the boundaries on which the prescribed values of stress $\bar{t}_{ni}$ and displacement $\bar{u}_i$ are imposed, respectively. For simplicity, we define $b_i = u_i|_{L^+} - u_i|_{L^-}$ on $L(= L^+ + L^-)$, where L is the union of all cracks, L^+ and L^- are defined in Fig. 4.

In a manner similar to that in Ref. [18], the total generalized potential energy for the crack problem defined above is given by

$$\Pi(\mathbf{b}) = \frac{1}{2}\int_L \mathbf{R}(\mathbf{b})\cdot\mathbf{b}_{,s}\,\mathrm{d}s - \int_\Gamma \bar{\mathbf{t}}\cdot\mathbf{b}\,\mathrm{d}s \tag{26}$$

where

$$\mathbf{b} = \{b_1\ b_2\}^{\mathrm{T}}; \qquad \mathbf{R} = \{R_1\ R_2\}; \qquad \bar{\mathbf{t}} = \{\bar{t}_{n1}\ \bar{t}_{n2}\} \tag{27}$$

with

$$R_i = \int \sigma_{ij}n_j\,\mathrm{d}s \qquad (i,j = 1,2) \tag{28}$$

As in the conventional BE method, the boundaries L and Γ are divided into a series of boundary elements for which the displacement discontinuity may be approximated by a linear function. To illustrate this, take a particular element m, which is a line connected by nodes m and $m+1$, as an example (Fig. 5).

$$\mathbf{b}(s) = \mathbf{b}_m F_m(s) + \mathbf{b}_{m+1}F_{m+1}(s) \tag{29}$$

With the approximation (29), the displacements can now be expressed in the form

$$\mathbf{u}(\mathbf{x}) = \sum_{m=1}^{M} \mathbf{U}_m\mathbf{b}_m \tag{30}$$

where M is the total number of nodes, $\mathbf{x} = \{x_1, x_2\}$, and

$$\begin{aligned} \mathbf{U}_m = &\frac{1}{l_{m-1}}\int_{l_{m-1}} \begin{bmatrix} U_{11} & U_{12} \\ U_{21} & U_{22} \end{bmatrix} s\,\mathrm{d}s \\ &+ \frac{1}{l_m}\int_{l_m} \begin{bmatrix} U_{11} & U_{12} \\ U_{21} & U_{22} \end{bmatrix} (l_m - s)\mathrm{d}s \end{aligned} \tag{31}$$

For the total potential energy (26), substitution of Eq. (29) into it yields

$$\Pi(\mathbf{b}) = \sum_{i=1}^{M} \mathbf{b}_i^T \left(\sum_{j=1}^{M} \mathbf{k}_{ij}\mathbf{b}_j/2 - \mathbf{g}_i\right) \tag{32}$$

where

$$\mathbf{k}_{ij} = \frac{1}{l_{j-1}}\int_{l_{j-1}} \begin{bmatrix} F_{11}^i & F_{12}^i \\ F_{12}^i & F_{22}^i \end{bmatrix} \mathrm{d}s - \frac{1}{l_j}\int_{l_j} \begin{bmatrix} F_{11}^i & F_{12}^i \\ F_{12}^i & F_{22}^i \end{bmatrix} \mathrm{d}s \tag{33}$$

$$\mathbf{g}_j = \frac{1}{l_{j-1}}\int_{l_{j-1}} \bar{\mathbf{t}}^{\mathrm{T}} s\,\mathrm{d}s + \frac{1}{l_j}\int_{l_j} \bar{\mathbf{t}}^{\mathrm{T}}(l_j - s)\mathrm{d}s \tag{34}$$

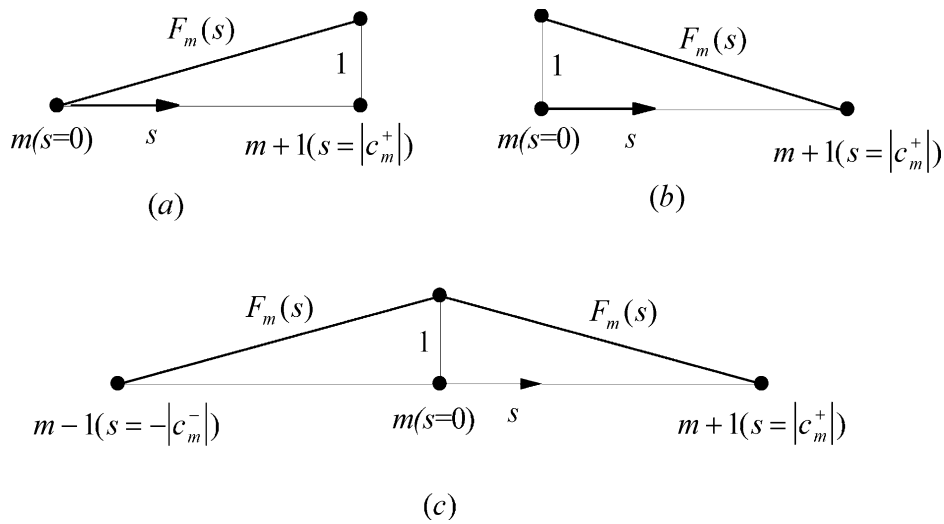

Fig. 5. Definitions for $F_m(s)$, $|c_m^+|$ and $|c_m^-|$.

with

$$F_{11}^i=\frac{1}{l_{i-1}}\int \mathrm{d}s\int_{l_{i-1}}[V_{111}(s,x)n_1+V_{121}(s,x)n_2]x\mathrm{d}x + \frac{1}{l_i}\int \mathrm{d}s\int_{l_i}[V_{111}(s,x)n_1+V_{121}(s,x)n_2](l_i-x)\mathrm{d}x \tag{35}$$

$$F_{12}^i=\frac{1}{l_{i-1}}\int \mathrm{d}s\int_{l_{i-1}}[V_{112}(s,x)n_1+V_{122}(s,x)n_2]x\mathrm{d}x + \frac{1}{l_i}\int \mathrm{d}s\int_{l_i}[V_{112}(s,x)n_1+V_{122}(s,x)n_2](l_i-x)\mathrm{d}x$$

$$F_{22}^i=\frac{1}{l_{i-1}}\int \mathrm{d}s\int_{l_{i-1}}[V_{221}(s,x)n_1+V_{222}(s,x)n_2]x\mathrm{d}x + \frac{1}{l_i}\int \mathrm{d}s\int_{l_i}[V_{221}(s,x)n_1+V_{222}(s,x)n_2](l_i-x)\mathrm{d}x$$

The minimization of Eq. (32) leads to a set of linear equations

$$\sum_{j=1}^{M}\mathbf{k}_{ij}\mathbf{b}_j=\mathbf{g}_i \tag{36}$$

The final form of the linear equations to be solved is obtained by selecting either Eq. (30) or Eq. (36). Eq. (30) will be chosen for those nodes at which displacements are prescribed, and Eq. (36) will be chosen for the remaining nodes.

3.2. Fibers

In this subsection, a two domain boundary element model is introduced for displacements and tractions on the boundary of each domain. The two subdomains are separated by the interfaces between fiber and matrix (Fig. 2(c)). Each subdomain can be separately modeled by direct BEM. A global assembly of the boundary element subdomains is then performed by forcing continuity of the displacements and tractions at the subdomain interface.

In two-dimensional linear elasticity, the BE formulation takes the form [19–22]

$$c^{(\alpha)}(\boldsymbol{\xi})u_i^{(\alpha)}(\boldsymbol{\xi}) = \int_{S^{(\alpha)}}[U_{ij}^{(\alpha)}(\mathbf{x},\boldsymbol{\xi})T_j^{(\alpha)}(\mathbf{x})-F_{ji}^{(\alpha)}(\mathbf{x},\boldsymbol{\xi})u_j^{(\alpha)}(\mathbf{x})]\mathrm{d}S(\mathbf{x}) \tag{37}$$

where the superscript (α) stands for the quantity associated with the αth phase, ($\alpha=1$ being matrix and $\alpha=2$ being fiber) and

$$S^{(\alpha)}=\begin{cases} S+\Gamma & \alpha=1 \\ S & \alpha=2 \end{cases}$$

$$c^{(\alpha)}(\boldsymbol{\xi})=\begin{cases} 1 & \text{if } \boldsymbol{\xi}\in\Omega^{(\alpha)} \\ 0.5 & \text{if } \boldsymbol{\xi}\in S^{(\alpha)}\ (S^{(\alpha)}\text{ smooth}) \\ 0 & \text{if } \boldsymbol{\xi}\notin\Omega^{(\alpha)}\cup S^{(\alpha)} \end{cases} \tag{38}$$

For plane strain the integral kernels G_{ij} and F_{ij} are given by

$$U_{ij}^{(\alpha)}(\mathbf{x},\boldsymbol{\xi})=\frac{1}{8\pi G^{(\alpha)}(1-\mu^{(\alpha)})} \times\left[(3-4\mu^{(\alpha)})\ln\left(\frac{1}{r}\right)\delta_{ij}+\frac{r_ir_j}{r^2}\right] \tag{39a}$$

$$F_{ji}^{(\alpha)}(\mathbf{x},\boldsymbol{\xi})=-\frac{1}{4\pi(1-\mu^{(\alpha)})r}\left\{(1-2\mu^{(\alpha)})\left(n_j\frac{r_i}{r}-n_i\frac{r_j}{r}\right) +\left[(1-2\mu^{(\alpha)})\delta_{ij}+\frac{2r_ir_j}{r^2}\right]\frac{r_n}{r}\right\} \tag{39b}$$

with

$$r_i=x_i-\xi_i,\quad r_n=r_in_i,\quad r=\sqrt{r_ir_i} \tag{40}$$

Eq. (39) can be used for plane stress if $\mu^{(\alpha)}$ is replaced by $\mu^{(\alpha)}(1-\mu^{(\alpha)})$.

To obtain a weak solution of Eq. (37) as in the conventional BEM, the boundary $S^{(\alpha)}$ is divided into

a series of boundary elements. After performing discretization using various kinds of boundary element (e.g. constant element, linear element, higher-order element) and collecting the unknown terms to the left-hand side and the known terms to the right-hand side, as well as using continuity conditions at the interface S (Fig. 2(b)), the boundary integral Eq. (37) becomes a set of linear algebraic equations

$$\mathbf{AY} = \mathbf{P} \tag{41}$$

where $\mathbf{Y}$ and $\mathbf{P}$ are the total unknown and known vectors, respectively, and $\mathbf{A}$ is the known coefficient matrix.

3.3. Holes

When the fiber in Fig. 2(c) becomes a hole, the boundary integral equation still holds true if one takes $\alpha = 1$ only. In this case the interfacial continuity condition is replaced by the hole boundary condition: $T_j = 0 (j = 1, 2)$ along the boundary S (Fig. 2(b)).

4. Periodic boundary conditions

Consider a rectangular unit-cell, as shown in Figs. 2 and 3, whose dimensions are a in x-direction and b in y-direction. The presence of periodically distributed inclusion phase results in periodic microscopic displacement and stress fields under remote uniform loads. Without loss of the generality, denote the periodic conditions of the displacement and stress fields by

$$u_i(\mathbf{y}) = u_i(\mathbf{y} + \mathbf{Y}) \qquad \forall \mathbf{y} \in \Omega \tag{42}$$

$$\sigma_{ij}(\mathbf{y}) = \sigma_{ij}(\mathbf{y} + \mathbf{Y}) \qquad \forall \mathbf{y} \in \Omega \tag{43}$$

where $\mathbf{Y} = (Y_1, Y_2, Y_3)$ is the vector of periodicity ($\mathbf{Y} = (a, b)$ in our analysis), Ω and Γ are again the domain and its boundary of the RVE, respectively. For illustration, Fig. 6 shows a typical periodic deformation of the composite. For any point, $\mathbf{y}^0$, located on the boundary Γ, the periodic displacement boundary condition of the RVE is

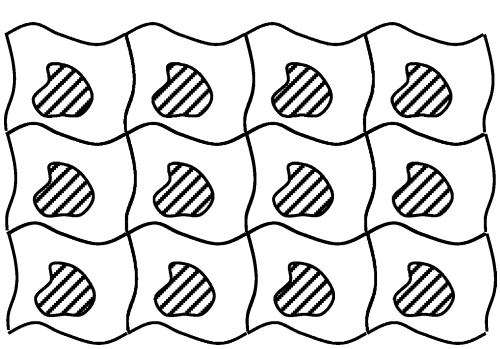

Fig. 6. A typical periodic deformation of composite.

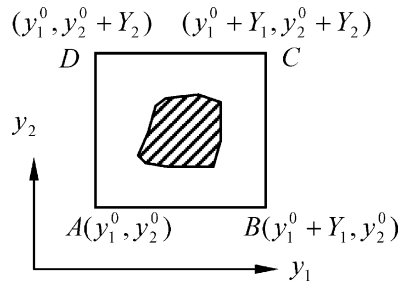

Fig. 7. The periodic RVE.

given by

$$u_i(\mathbf{y}^0) = u_i(\mathbf{y}^0 + \mathbf{Y}), \qquad \forall \mathbf{y}^0 \in \Gamma \tag{44}$$

The stress periodicity of the RVE requires an anti-periodic traction boundary condition

$$T_i(\mathbf{y}^0) = -T_i(\mathbf{y}^0 + \mathbf{Y}), \qquad \forall \mathbf{y}^0 \in \Gamma \tag{45}$$

For a two-dimensional rectangular RVE, as shown in Fig. 7, for example, the periodic displacement boundary conditions are expressed by

$$u_1(y_1^0, y_2) = u_1(y_1^0 + Y_1, y_2) \tag{46a}$$

$$u_2(y_1^0, y_2) = u_2(y_1^0 + Y_1, y_2) \tag{46b}$$

for the left and right sides, and

$$u_1(y_1, y_2^0) = u_1(y_1, y_2^0 + Y_2) \tag{47a}$$

$$u_2(y_1, y_2^0) = u_2(y_1, y_2^0 + Y_2) \tag{47b}$$

for the upper and lower sides (Fig. 7). The anti-periodicity of the traction boundary conditions yields

$$\sigma_{11}(y_1^0, y_2) = -\sigma_{11}(y_1^0 + Y_1, y_2) \tag{48a}$$

$$\sigma_{12}(y_1^0, y_2) = -\sigma_{12}(y_1^0 + Y_1, y_2) \tag{48b}$$

for the left and right sides and

$$\sigma_{22}(y_1, y_2^0) = -\sigma_{22}(y_1, y_2^0 + Y_2) \tag{49a}$$

$$\sigma_{21}(y_1, y_2^0) = -\sigma_{21}(y_1, y_2^0 + Y_2) \tag{49b}$$

for the upper and lower sides. In the case of symmetric RVE, the periodic boundary conditions can be reduced to ordinary boundary conditions [23–25]. The periodic boundary conditions described above can easily be implemented into a standard boundary element program, because the boundary tractions and boundary displacements are the basic variables in BEM.

5. Numerical comparison between BEM and FEM

As a numerical illustration of the proposed approach, the example of a square RVE with a circular rigid fiber was analyzed. The Poisson's ratio of the matrix used in the present example is 0.35. Some numerical results were obtained and comparison is made with those from the FE

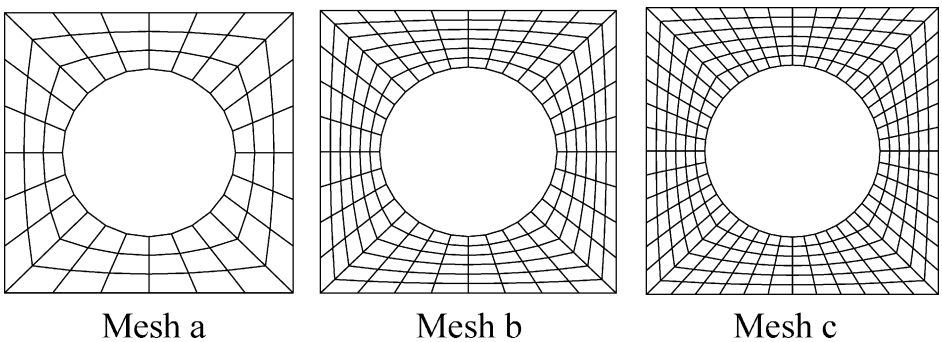

Fig. 8. Three meshes of FE and BE for convergence study.

Table 1
Numerical result for different meshes

	Mesh a	Mesh b	Mesh c
D_{1111}/E_0	3.34642	3.34643	3.34643
D_{1122}/E_0	1.31500	1.31501	1.31500

method. For simplicity, it is assumed that the rigid fiber has infinite length so that it can be treated as plane strain problem. When a specific uni-axial strain state (generally unit strain for simplicity) is applied in a unit-cell, the average stresses are calculated by BEM or FEM. Then the plane-strain stiffness coefficients of the composite can be obtained.

Both the BEM and FE calculations are carried out for numerical comparison. In the finite element model, the 8-node quadratic element is employed. The BEM model uses the mesh on the boundary of the finite element model. To study the convergence, three meshes of the BEM and FEM are used, as shown in Fig. 8. They have 48 boundary elements and 96 nodes, 64 boundary elements and 128 nodes, and 96 boundary elements and 192 nodes, respectively. The calculated effective stiffness coefficients of the composite are listed in Table 1 for the three meshes. It is shown that the stiffness coefficients are insensitive to the meshes and a good convergence is demonstrated.

The results obtained from both the FE method and BEM with Mesh b are listed in Figs. 9–11. Present composite is transversely isotropic elastic body. The effective engineering constants can be calculated through the plane-strain stiffness matrix by

$$\mu = \frac{D_{1111}}{D_{1111} + D_{1122}} \tag{50a}$$

$$E = \frac{D_{1111}(1+\mu)(1-2\mu)}{1-\mu} \tag{50b}$$

$$G = D_{1212} \tag{50c}$$

where E, μ and G are Young's modulus, Poisson's ratio and shear modulus, respectively.

Fig. 9 shows the Young's modulus as a function of the inclusion volume fraction. It is seen that the two methods lead to very similar results. A lower bound of the Young's modulus obtained from the Reuss approximation [3,5] is also plotted in Fig. 9 for numerical comparison. The effective Poisson's ratio vs inclusion volume fraction is shown in Fig. 10, where the results from BEM and FE method are seen to agree within plotting accuracy. Fig. 11 plots the variation of the effective shear modulus with the inclusion volume fraction. It is evident that for composite reinforced by rigid inclusion, the Young's modulus and shear modulus increase along with the increase of inclusion volume fraction, while the Poisson's ratio decreases with

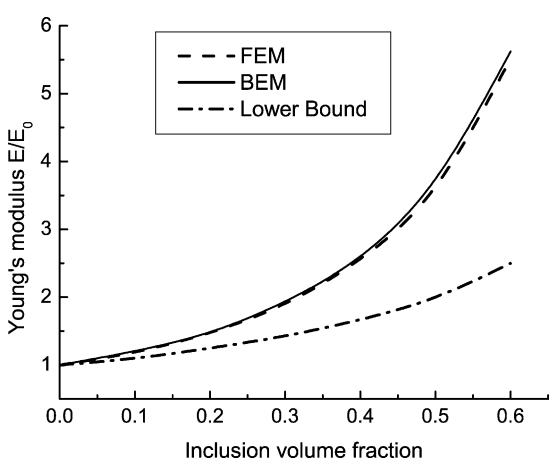

Fig. 9. Young's modulus vs inclusion volume fraction.

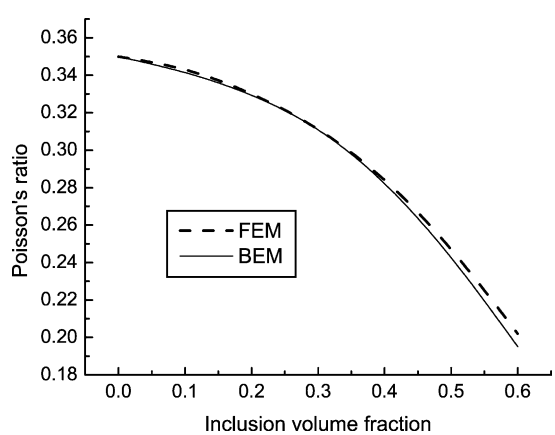

Fig. 10. Poisson's ratio vs inclusion volume fraction.

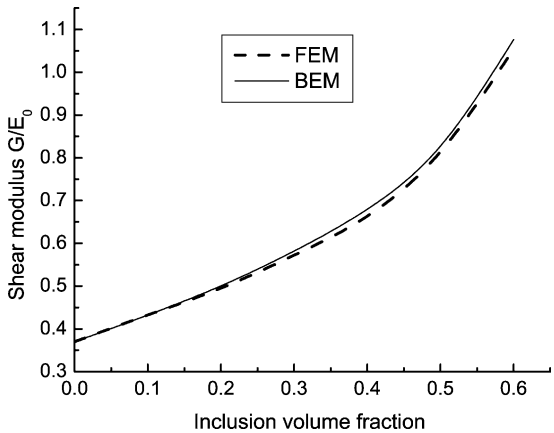

Fig. 11. Shear modulus vs inclusion volume fraction.

the increase of inclusion volume fraction. More numerical examples are expected following this approach and will be reported elsewhere.

6. Conclusions

A BEM-based micro-mechanics model for composites with periodic inclusions or defects is presented for estimating overall elastic properties. The proposed formulation is capable of modeling two-phase composites with inhomogeneities such as cracks, holes or inclusions. The study indicates that the boundary field values of a RVE are sufficient for calculation of the effective properties of the two-phase composites mentioned above. As a consequence, the calculation of internal fields can be omitted. It is also indicated that the periodic boundary condition can be easily implemented by the BEM program. The numerical example shows that the results from BEM are in agreement with those by FE method, but with less degree of freedom.

References

[1] Eshelby JD. The determination of the elastic field of an ellip-soidal inclusion and related problems. Proc R Soc Lond 1957;A241: 376–96.
[2] Hashin Z. Analysis of composite materials—a survey. J Appl Mech 1983;50:481–505.
[3] Mura T. Micromechanics of defeats in solids, 2nd Revised ed. Dordrecht: Martin Nijhoff Publishers; 1987.
[4] Nemat-Nasser S, Hori M. Micromechanics: overall properties of heterogeneous materials. Amsterdam: North Holland Publishers; 1993.
[5] Christensen RM. Mechanics of composite materials. New York: Wiley; 1979.
[6] Christman T, Needleman A, Suresh S. An experimental and numerical study of deformation in metal-ceramic composites. Acta Metall Mater 1989;37:3029–50.
[7] Tvergarrd V. Analysis of tension properties for a whisker-reinforced metal matrix composite. Acta Metall Mater 1990;38:185–94.
[8] Yang Q-S, Qin Q-H. Fiber interactions and effective elasto-plastic properties of short-fiber composites. Compos Struct 2001;54(4):223–8.
[9] Papathanasiou TD, Ingber MS, Guell DC. Stiffness enhancement in aligned, short-fibre composites: a computational and experimental investigation. Compos Sci Technol 1995;54:1–9.
[10] Jiang ZQ, Chandra A, Huang Y. A hybrid micro–macro BEM with micro-scale inclusion-crack interactions. Int J Solids Struct 1995;33: 2309–39.
[11] Herding U, Kuhn G. A field boundary element formulation for damage mechanics. Engng Anal Bound Elem 1996;18:137–47.
[12] Fotiu PA, Heuer R, Ziegler F. BEM analysis of grain boundary sliding in polycrystals. Engng Anal Bound Elem 1995;15:349–58.
[13] Qi N, Phan-Thien N, Fan XJ. Effective moduli of particulate solids: the completed double layer boundary element method with lubrication approximation. Z Angew Math Phys 2000;51:92–113.
[14] Hohe J, Becker W. An energetic homogenization procedure for elastic properties of general cellular sandwich cores. Composites, Part B 2001;32:185–97.
[15] Hill R. Elastic properties of reinforced solids: some theoretical principles. J Mech Phys Solids 1963;11:357–72.
[16] Hazanov S. Hill condition and overall properties of composites. Arch Appl Mech 1998;68:385–94.
[17] Nabarro FRN. Theory of crystal dislocations. Oxford: Oxford University Press; 1967.
[18] Qin QH, Yu SW. Fracture and damage analysis of a cracked body by a new boundary element model. Communications in Numerical Methods in Engineering 1997;13:327–36.
[19] Brebbia CA, Telles JCF, Wrobel LC. Boundary element techniques. Berlin: Springer; 1984.
[20] Banerjee PK, Butterfield R. Boundary element methods in engineering science. London: McGraw-Hill; 1981.
[21] Crouch SL, Starfield AM. Boundary element methods in solid mechanics. London: George Allen and Unwin Ltd; 1983.
[22] Brebbia CA, Venturini WS. Boundary element techniques: applications in stress analysis and heat transfer. Southampton: Computational Mechanics Publications; 1987.
[23] Anthoine A. Derivation of the in-plane elastic characteristics of masonry through homogenization theory. Int J Solids Struct 1995;32: 137–63.
[24] Hassani B, Hinton E. A review of homogenization and topology Optimization. I-Homogenization theory for media with periodic structure, p. 707–17;. II-Analytical and numerical solution of homogenization equations, p. 719–38, Comput Struct 1998; 69.
[25] Miehe C, Koch A. Computational micro-to-macro transitions of discretized microstructures undergoing small strains. Arch Appl Mech 2002;72:300–17.